

# Measurement of the $t\bar{t}$ Cross Section in the Lepton Plus Jets Channel Using Neural Networks in $4.6 \text{ fb}^{-1}$ of CDF data.

The CDF Collaboration  
URL <http://www-cdf.fnal.gov>  
(Dated: September 25, 2009)

We present a measurement of the top pair production cross section in  $p\bar{p}$  collisions at 1.96 TeV, with an integrated luminosity of  $4.6 \text{ fb}^{-1}$  at the CDF experiment on the Fermilab Tevatron. We use a neural network technique to discriminate between top pair production and background processes in a sample of events with an isolated, energetic lepton, large missing transverse energy and three or more energetic jets. We then significantly reduce the dependence on the luminosity measurement and its associated large systematic uncertainty. We compute the ratio of the  $t\bar{t}$  to the  $Z$  cross section, measured using the same triggers and dataset, and then multiplying this ratio by the theoretical  $Z$  cross section. We measure a top pair production cross section of  $\sigma_{t\bar{t}} = 7.63 \pm 0.37(\text{stat}) \pm 0.35(\text{syst}) \pm 0.15(\text{theory}) \text{ pb}$  for a top mass of  $172.5 \text{ GeV}/c^2$ , which corresponds to a total uncertainty of 7.0%.

*Preliminary Results for Summer 2009 Conferences*

## I. INTRODUCTION

Since the discovery of the top quark [1], experimental attention has turned to the examination of its properties. Within the context of the Standard Model, in  $p\bar{p}$  collisions top quarks are produced in pairs through the strong interaction, via  $q\bar{q}$  annihilation (85%) and gluon fusion (15%) at  $\sqrt{s} = 1.96$  TeV. Recent theoretical calculations constrain the top pair production cross section with an uncertainty of the order of 9% [2–4]. The top quark is expected to decay to a W boson and  $b$  quark nearly 100% of the time. The W boson subsequently decays to either a pair of quarks or a lepton-neutrino pair. Measuring the rate of the reaction  $p\bar{p} \rightarrow t\bar{t} \rightarrow \ell\bar{\nu}_\ell q\bar{q}' b\bar{b}$ , the lepton+jets channel, tests both the production and decay mechanisms of the top quark.

This note describes a measurement of the top pair production cross section in the lepton+jets channel at  $\sqrt{s} = 1.96$  TeV. We develop a neural network technique to maximize the discriminating power from kinematic and topological variables. The sensitivity of the neural network technique is comparable to that for the traditional CDF secondary vertex  $b$ -tag method [5, 6], which suppresses the dominant background from  $W$ +jets at a cost of a 45% loss in signal efficiency. This kinematic method then allows us to check the assumptions in the  $b$ -tag method and test the modeling of signal and background processes with higher statistics. Exploring the top cross section in many different channels and using many different assumptions is important for looking for signs of new physics as new physics might appear differently in the various channels. An excellent understanding of top pair production and  $W$ +jets background kinematics is required for the searches for the Higgs boson and new physics signatures at both the Tevatron and the LHC.

The  $t\bar{t}$  cross section measurement, using this method, is systematics dominated. The largest systematic is due to the uncertainty on the luminosity determination which is 5.8%. In order to significantly reduce this uncertainty we can exploit the correlation between the luminosity measurements in two different processes; in this case the  $t\bar{t}$  and  $Z$  cross sections are used. By taking the ratio of the  $t\bar{t}$  and  $Z$  cross sections, the luminosity uncertainty almost entirely cancels out. By then multiplying this ratio by the best theoretical calculation of the  $Z$  cross section, a  $t\bar{t}$  cross section can be obtained. In effect, one is replacing the luminosity uncertainty with the theoretical and experimental uncertainties on the  $Z$  cross section, both of which are rather small.

## II. DATA SAMPLE AND EVENT SELECTION

This analysis is based on a sample of integrated luminosity of  $4.6 \text{ fb}^{-1}$  collected with the CDF II detector. The CDF detector is described in detail in [7]. This analysis uses the standard CDF lepton+jets event selection. The data are collected with an inclusive lepton trigger that requires an electron or muon with  $E_T \geq 18$  GeV ( $p_T \geq 18$  GeV/ $c$  for the muon). From this inclusive lepton dataset we select offline events with a reconstructed isolated electron  $E_T$  (muon  $p_T$ ) greater than 20 GeV, missing transverse energy ( $\cancel{E}_T$ )  $\geq 20$  GeV and at least 3 jets with  $E_T \geq 20$  GeV. On top of this basic selection we apply 2 further cuts to suppress the multi-jet background: the leading jet must have an  $E_T \geq 35$  GeV and require also that  $\cancel{E}_T \geq 35$  GeV.

### A. $t\bar{t}$ Acceptance

The total acceptance is measured using a combination of data and Monte Carlo. The geometric times kinematic acceptance of the event selection is measured using the PYTHIA Monte Carlo program [8]. A top mass of  $175 \text{ GeV}/c^2$  is used for the acceptance determination. The efficiency for identifying the isolated, high  $p_T$  lepton is scaled to the value measured in the data using the unbiased leg in  $Z$ -boson decays. Table I summarizes the observed number of data events and the expected number of  $t\bar{t}$  events assuming a cross section of 7.45 pb.

Jet multiplicity	$W \rightarrow e\nu$	$W \rightarrow \mu\nu$	Total	Expected $t\bar{t}$
$W+ \geq 3$	5119	3504	8623	1193

TABLE I: The observed number of W candidate events and the expected number of  $t\bar{t}$  events, assuming a theoretical cross section of 7.45 pb at a top mass of  $172.5 \text{ GeV}/c^2$ .

## B. Backgrounds

The events selected by the cuts mentioned above are dominated by QCD production of  $W$  bosons with multiple jets. Much theoretical progress has been made recently to improve the description of the  $W$ +jets process, with leading-order matrix element generators now available to describe the parton hard scattering for processes with a  $W$  and up to six additional partons in the final state. We use the ALPGEN [9] matrix element generator, convoluted with the CTEQ5L parton distribution functions [11]. We require parton  $p_T \geq 8$  GeV/ $c$ ,  $|\eta| \leq 3.0$  and minimum separation  $\Delta R \geq 0.2$  for  $u$ ,  $d$ ,  $s$  and  $g$  partons. We have verified that the shapes of the kinematic distributions used in our kinematic analysis are not sensitive to these values. We choose a default momentum transfer scale of  $Q^2 = M_W^2 + \sum_i p_{T,i}^2$  for the parton distribution functions and the evaluation of  $\alpha_s$ , where  $p_{T,i}$  is the transverse momentum of the  $i$ -th parton. We use the PYTHIA parton shower algorithm to evolve the final state partons to colorless hadrons. For this analysis, we combine the  $W + n$  where  $n=0,1,..,4$ , parton ALPGEN+PYTHIA Monte Carlo samples to obtain the full kinematic distributions. The dominant contributions come from the  $W+3p$  and  $W+4p$  samples. These samples are used to model all electroweak backgrounds. The previous version of this analysis [12] showed that the kinematic distributions of these other backgrounds are very similar to the  $W$ +jets samples. We consider a 1% systematic due to this assumption.

The other substantial background in this analysis comes from events without  $W$  bosons. These events are typically QCD multi-jet events where one jet has faked a high- $p_T$  lepton and mis-measured energies produce apparent  $\cancel{E}_T$ . We model the kinematics of this background by using those events that pass all of our selection requirements but come through dijet triggers instead of high  $p_T$  lepton triggers. We estimate the rate of such events from a fit to the  $\cancel{E}_T$  distribution after all cuts but the  $\cancel{E}_T$  cut are applied. The QCD background will have predominantly low  $\cancel{E}_T$  with tails extending into the signal region. Figure 1 shows the  $\cancel{E}_T$  distributions used for this fit. In this fit the top cross section is constrained to 7.45 pb. This fit tells us that we expect approximately 448 QCD events. A 50% relative systematic uncertainty is taken on the number of QCD events. In the final fit, the QCD fraction is constrained to the value obtained by this fit with an uncertainty of 50%.

## III. $t\bar{t}$ CROSS SECTION MEASUREMENT METHOD

A comparison of the observed data events with the expected number of  $t\bar{t}$  signal events in Table I indicates the expected signal to background ratio is about 1:4.5 in the  $W + \geq 3$  sample. At such low signal purities, the sensitivity to top pair production from the observed number of events alone is eradicated by the large uncertainty on the leading-order theoretical prediction for  $W$ +jets background. Other CDF measurements of the top pair production cross section have used  $b$ -tagging, with 55% signal efficiency, to improve the signal-to-background ratio to 2:1 and 3:1, in the  $W + \geq 3$  jets and  $W + \geq 4$  jets respectively, and also use the more accurate prediction for the fraction of  $W$ +jets containing heavy flavor.

This analysis instead exploits the discrimination available from kinematic and topological variables to distinguish top pair production from background. Due to the large mass of the top quark, top pair production is associated with central, spherical, energetic events with different kinematics from the predominantly lower energy background processes. We consider separately two background components: electroweak processes modelled by the  $W$ +jets Monte Carlo, and multi-jet QCD processes obtained from data. To maximize our discriminating power, we use an Artificial Neural Network (ANN) technique [14]. ANNs employ information from several variables while accounting for the correlations among them.

The expected number of events in the  $i$ -th bin of the NN output is given by

$$n_i = (\sigma_{t\bar{t}} \cdot \frac{\epsilon_{t\bar{t}}}{\mathcal{L}} P_{t\bar{t},i} + n_w P_{w,i} + n_q P_{q,i}), \quad (1)$$

where  $P_{t\bar{t},i}$ ,  $P_{w,i}$ ,  $P_{q,i}$  are the probability of observing an event in bin  $i$  from  $t\bar{t}$ ,  $W$ -like and multi-jet processes.  $\epsilon_{t\bar{t}}$  is the acceptance estimate including the branching ratio for  $W \rightarrow \ell\nu$ , and  $\mathcal{L}$  the luminosity measurement.  $n_i$  denotes the number of observed data events that populate the  $i$ -th bin.  $\sigma_{t\bar{t}}$ ,  $n_w$ ,  $n_q$  are the parameters of the fit, representing the  $t\bar{t}$  cross-section, the number of  $W$ -like and multi-jet events respectively present in the sample. The level of the multi-jet background,  $n_q$  is fixed to that expected from the fit to the  $\cancel{E}_T$  distribution with an uncertainty of 50%. We perform a binned likelihood fit to the discriminating variable and find the most likely number of events from  $t\bar{t}$  production,  $n_{t\bar{t}}$

$$L(\sigma_{t\bar{t}}, n_w, n_q) = \prod_{i=1}^{N_{data}} \frac{e^{-n_i} n_i^{d_i}}{d_i!}, \quad (2)$$

## A. Neural Network

The Neural Network method used for the previous version of this analysis was maintained. There are many algorithms one could use for adjusting the weights in order to produce an optimized network [15]. For this particular problem, the previous version of this analysis, obtained satisfactory results by using the default JETNET back-propagation training method with a term added to the error function in order to discourage large weights. The same 7 inputs to the ANN were chosen for this analysis. The variables of choice are shown in Tab. II

Variable	Definition
$H_T$	Scalar sum of transverse energies of jets, lepton and $\cancel{E}_T$ .
Aplanarity	$3/2 \cdot Q_1$
$\Sigma p_z / \Sigma E_T$	Ratio of total jet longitudinal momenta to total jet transverse energy.
$\min(M_{jj})$	Minimum di-jet invariant mass
$\eta_{max}$	Maximum $\eta$ of jet.
$\Sigma_{i=3}^5 E_{T,i}$	Sum $E_T$ of third, fourth and fifth jets.
$\min(\Delta R_{jj})$	Minimum di-jet separation in $\eta - \phi$ plane.

TABLE II: Definition of variables used as inputs to the ANN this analysis. The momentum tensor of the event is formed from the lepton,  $\cancel{E}_T$  and the  $E_T$  of the five highest  $E_T$  jets. The eigenvalues are ordered such that  $Q_1 \leq Q_2 \leq Q_3$ .

The ANN is a feed-forward perceptron with one intermediate (hidden) layer and one output node. For training, we use 5000 PYTHIA  $t\bar{t}$  and 5000 ALPGEN+PYTHIA  $W$ + $n$ jets (where  $n$  in this case is 3 or 4 depending on the number of jets in the event) Monte Carlo events and require an output of 1.0 for  $t\bar{t}$  signal and 0.0 for  $W$ +jets background. Other sources of background are not considered during the training process. The weights of the network are adjusted to minimize a typical mean squared error function:

$$E = \frac{1}{N} \sum_i^N (O_i - t_i)^2$$

where  $O_i$  is the output of the network for the input event  $i$  and  $t_i$  is the desired target value. Learning is an iterative process and we use an independent testing sample of 1900 PYTHIA  $t\bar{t}$  and 1900 ALPGEN+PYTHIA  $W$ +jets Monte Carlo to evaluate the ANN performance and choose when to stop training. After training was completed, an independent validation sample was used to check the quality of the training.

## IV. SYSTEMATIC UNCERTAINTIES

Systematic uncertainties in this analysis come from Monte Carlo modeling of the geometrical and kinematic acceptance for signal, the luminosity measurement, and from modeling of the kinematic shapes for signal and background. The list of the systematic uncertainties we have considered for the  $t\bar{t}$  cross section is summarized in Table III. The first column of numbers refer to this measurement.

For the sources of systematic uncertainties affecting the shape of the kinematic distributions, 10'000 pseudo-experiments (PE) are thrown using the shifted templates (both shape and normalisation are changed when relevant). We fit the PE using the nominal templates. Note that for the systematics that affect the  $W$ +jets, as the normalisation is left to float in the fit, the only systematic effect considered is that of the shape. The systematics affecting the shape of the  $W$ +jets are: the jet energy scale (JES) and interaction scale ( $Q^2$ ).

The largest source of systematic uncertainty comes from the jet energy scale. The JES uncertainty comes from the uncertainty on the jet energy corrections for different calorimeter response (as a function of  $\eta$ ), the absolute hadron energy scale, and fragmentation etc. This affects simultaneously five of the seven kinematic variables used in the ANN analysis.

The next largest uncertainty, denoted  $t\bar{t}$  generator uncertainty in Tab. III is due to the difference in the fitted  $t\bar{t}$  cross section when comparing the signal modelling from HERWIG and from PYTHIA Monte Carlo. The kinematic distributions do not seem to be very different but there is a significant change in acceptance between these two samples.

The initial- and final-state radiation uncertainties (IFSR) on  $t\bar{t}$  are estimated by increasing and decreasing simultaneously the parton shower evolution parameters by an amount based on studies of the CDF Drell-Yan data. The effect of the interaction scale variation,  $Q^2$ , on the W+jets background is estimated using a new CDF prescription for varying some ALPGEN parameters. The PDF uncertainties on  $t\bar{t}$  are obtained by considering 21 sets PDF eigenvectors along with variations on the coupling constant  $\alpha_s$ . Uncertainties on the QCD background modeling include changing the input normalisation by a factor of 2 as well as comparing the default model with a model obtained from events that fail 2 out of the 5 electron identification cuts.

The luminosity measurement of  $2.8 \text{ fb}^{-1}$  has an uncertainty of 5.8%, of which 4.2% comes from the acceptance and operation of the luminosity monitor and 4.0% from the calculation of the total  $p\bar{p}$  cross section [16].

Effect	Top Cross section		Z Cross section		Ratio = $\sigma_{t\bar{t}}/\sigma_Z$		
	Upwards shift	Downwards shift	Upwards shift	Downwards shift	Upwards shift	Downwards shift	Uncertainty
Statistical top	-4.82	+4.88	+0.00	+0.00	-4.82	+4.88	4.85
Statistical Z	+0.00	+0.00	-0.32	+0.32	-0.32	+0.32	0.32
Jet $E_T$ Scale	-2.90	+2.93	+0.00	+0.00	-2.90	+2.93	2.91
W+jets $Q^2$ Scale	+0.25	-2.41	+0.00	+0.00	-1.33	+1.33	1.33
Z+jets $Q^2$ Scale	+0.00	+0.00	-0.20	+0.34	-0.27	+0.27	0.27
$t\bar{t}$ IFSR	-0.63	+0.21	+0.00	+0.00	-0.42	+0.42	0.42
QCD shape	-0.48	+0.48	+0.00	+0.00	-0.48	+0.48	0.48
QCD fraction	+0.56	-1.05	+0.00	+0.00	-0.81	+0.81	0.81
$t\bar{t}$ generator	-2.50	+2.50	+0.00	+0.00	-2.50	+2.50	2.50
$t\bar{t}$ gen. branching ratio	-0.21	+0.95	+0.00	+0.00	-0.21	+0.95	0.58
$t\bar{t}$ PDF	-0.31	+0.45	-1.39	+1.24	-0.79	+1.10	0.94
$t\bar{t}$ Colour Reconnection	-0.16	+0.16	+0.00	+0.00	-0.16	+0.16	0.16
Other EWK	-1.00	+1.00	+0.00	+0.00	-1.00	+1.00	1.00
MC statistics	+0.00	+0.00	-0.14	+0.14	-0.14	+0.14	0.14
CEM ID SF	+0.35	-0.35	+0.83	-0.80	-0.48	+0.46	0.47
CMUP ID SF	+0.29	-0.29	+0.32	-0.32	-0.03	+0.03	0.03
CEM trigger efficiency	+0.27	-0.27	+0.02	-0.02	-0.25	+0.25	0.25
CMUP trigger efficiency	+0.45	-0.44	+0.05	-0.05	-0.39	+0.39	0.39
$Z_{vtx}$ SF	+0.21	-0.21	+0.21	-0.21	-0.00	+0.00	0.00
nJet (NLO)	+0.00	+0.00	+0.02	-0.02	-0.02	+0.02	0.02
CEM energy Scale	+0.00	+0.00	-0.08	+0.08	-0.08	+0.08	0.08
CMUP energy Scale	+0.00	+0.00	-0.02	+0.02	-0.02	+0.02	0.02
Z Background	+0.00	+0.00	-0.04	+0.04	-0.04	+0.04	0.04
Track ID	+0.00	+0.00	+0.61	-0.60	-0.61	+0.60	0.60
Luminosity	+6.16	-5.48	+6.57	-5.21	-0.39	+0.00	0.19
Total sys. before lumi.	-4.16	+4.97	-1.82	+1.72	-4.49	+4.67	4.56
Total systematic	-7.43	+7.40	-6.82	+5.48	-4.51	+4.67	4.57
Total uncertainty	-8.86	+8.86	-6.82	+5.48	-6.60	+6.75	6.66

TABLE III: Table for systematic errors for the  $t\bar{t}$  and Z cross section measurements as well as the ratio of the two. The overall uncertainty is obtained by adding in quadrature the individual effects.

## V. MEASUREMENT OF THE $t\bar{t}$ CROSS SECTION USING THE RATIO OVER THE Z CROSS SECTION

In order to significantly reduce the dominant source of systematic uncertainty, we measure the ratio of the  $t\bar{t}$  to Z cross sections using the same dataset and triggers.

The Z cross section measurement is relatively sensitive to the PDFs used. Moreover, the dominant systematic uncertainty is due to the uncertainties on the PDFs. For these reasons, the MC signal samples for Z and  $t\bar{t}$  are re-weighted from the CTEQ5L Leading Order (LO) PDF sets they were generated with to the more recent CTEQ6.6 Next to Leading Order (NLO) PDF sets. The PDF uncertainty considered for this part of the analysis is the uncertainty due to the CTEQ6.6 error eigenvector variations as well as  $\pm 1\sigma$  variations on the value of  $\alpha_s$ , as implemented in CTEQ6AB. These two sources of uncertainties are added in quadrature.

For  $t\bar{t}$  events in 3 or more jets, assuming a top mass of  $172.5 \text{ GeV}/c^2$  we measure a cross section with the artificial Neural Network technique of

$$\sigma_{t\bar{t}} = 7.52 \pm 0.36(stat) \pm 0.34(sys) \pm 0.44(lumi)pb. \quad (3)$$

where the first uncertainty is statistical, the second is systematic excluding the luminosity and the third is the luminosity uncertainty. These results are in good agreement with the theoretical prediction of  $7.45 \text{ pb}$  for a top mass of  $172.5 \text{ GeV}/c^2$ . The expected statistical sensitivity was estimated using  $10^4$  pseudo-experiments and was found to be consistent with the value obtained from data. The NN output distribution used for the final fit is shown in Figure 2.

The  $Z$  cross section is then measured using central electron and muon pairs, the same data samples as used for the  $t\bar{t}$  cross section. The selected  $Z$  sample has very little background and the systematics are dominated by the uncertainty due to the PDFs. The cross section is measured in data in the mass window of  $66 - 116 \text{ GeV}/c^2$ . The central value is then re-weighted from the CTEQ5L to the CTEQ6.6 PDFs. A small correction factor is applied to account for the virtual photon contribution as well as the finite mass window used in the analysis. The resulting  $Z$  cross section is measured to be

$$\sigma_Z = 247.79 \pm 0.79(stat) \pm 4.38(sys) \pm 14.59(lumi)pb. \quad (4)$$

By taking the ratio of the  $t\bar{t}$  to the  $Z$  cross sections, the uncertainty due to the luminosity almost entirely cancels out. The systematic uncertainties are treated with their appropriate correlations between the two measurements and can be found in the last column of Tab. III.

From this ratio, one can obtain a value for the  $t\bar{t}$  cross section by multiplying the ratio  $R$  by the best theoretical calculation of the  $Z$  cross section. The final  $t\bar{t}$  cross section is thus given by

$$\sigma_{t\bar{t}} = R \cdot \sigma_Z^{theory}. \quad (5)$$

The theoretical cross section used is

$$\sigma_Z^{theory} = 251.3 \pm 5.0(sys)pb. \quad (6)$$

In this case the systematics between  $R$  and the theoretical calculation are taken to be uncorrelated; The PDF uncertainties are found to be uncorrelated between the theoretical calculation and the ratio  $R$ .

We thus obtain the final result of this measurement

$$\sigma_{t\bar{t}} = 7.63 \pm 0.37(stat) \pm 0.35(sys) \pm 0.15(Z theory)pb. \quad (7)$$

The total uncertainty on this measurement is 7.0%, with the dominant systematic uncertainty being the jet energy scale.

### A. Results as a Function of the Assumed Top Mass

In order to obtain the results for the top cross section for different mass points, we carry out the identical fit as done with the central mass point of  $172.5 \text{ GeV}/c^2$  but using the MC corresponding to the new mass point. Note that only the statistical uncertainty is re-calculated. The systematics are not re-computed for each mass point. We measure two different mass points around the nominal: 170 and 175  $\text{GeV}/c^2$ . The results are

$$\sigma_{t\bar{t}bar}(M = 170) = 8.33 \pm 0.40(stat) \pm 0.39(sys) \pm 0.17(Z theory)pb, \quad (8)$$

and

$$\sigma_{t\bar{t}bar}(M = 175) = 7.29 \pm 0.35(stat) \pm 0.34(sys) \pm 0.14(Z theory)pb, \quad (9)$$

for those two mass points, respectively.

## VI. CONCLUSIONS

The  $t\bar{t}$  cross section has been measured in the lepton+jets channel using  $4.6 \text{ fb}^{-1}$  of CDF data. A fit to a NN output relying on the kinematics of the event was performed. The largest uncertainty, due to the luminosity measurement, almost entirely cancels out by computing the ratio of the  $t\bar{t}$  to the  $Z$  cross section and then multiplying the ratio by the best theoretical estimate of the  $Z$  cross section. The luminosity uncertainty is essentially replaced by a PDF uncertainty on the experimental  $Z$  cross section as well as by a theoretical uncertainty on the calculated  $Z$  cross section. The measured cross  $t\bar{t}$  cross section is

$$\sigma_{t\bar{t}} = 7.63 \pm 0.37(\text{stat}) \pm 0.35(\text{sys}) \pm 0.15(Z \text{ theory})\text{pb}. \quad (10)$$

The total uncertainty is 7.9%.

## Acknowledgments

We thank the Fermilab staff and the technical staffs of the participating institutions for their vital contributions. This work was supported by the U.S. Department of Energy and National Science Foundation; the Italian Istituto Nazionale di Fisica Nucleare; the Ministry of Education, Culture, Sports, Science and Technology of Japan; the Natural Sciences and Engineering Research Council of Canada; the National Science Council of the Republic of China; the Swiss National Science Foundation; the A.P. Sloan Foundation; the Bundesministerium für Bildung und Forschung, Germany; the Korean Science and Engineering Foundation and the Korean Research Foundation; the Science and Technology Facilities Council and the Royal Society, UK; the Institut National de Physique Nucleaire et Physique des Particules/CNRS; the Russian Foundation for Basic Research; the Ministerio de Ciencia e Innovación, and Programa Consolider-Ingenio 2010, Spain; the Slovak R&D Agency; the Academy of Finland; and the Royal Society of Edinburgh/Scottish Executive Support Research Fellowship.

- 
- [1] CDF Collaboration, F.Abe *et al.*, Phys. Rev. Lett. **74** 2626 (1995); D0 Collaboration, S. Abachi *et al.*, Phys. Rev. Lett. **74**, 2632 (1995).
  - [2] M. Cacciari, S. Frixione, M. L. Mangano, P. Nason and G. Ridolfi, [arXiv:0804.2800] (2008) and JHEP **0404**, 068 (2004) [arXiv:hep-ph/0303085].
  - [3] N. Kidonakis and R. Vogt, [arXiv:0805.3844] (2008) and Phys. Rev. D **68** 114014 (2003).
  - [4] S. Moch and P. Uwer, [arXiv:0807.2794] (2008).
  - [5] CDF collaboration, "Measurement of the Top Pair Cross Section in the Lepton plus Jets decay channel with  $2.7 \text{ fb}^{-1}$ ", CDF public note 9462
  - [6] CDF collaboration, "Measurement of the  $t\bar{t}$  productin cross section in  $p\bar{p}$  collisions at  $\sqrt{s} = 1.96 \text{ TeV}$  using Lepton+Jets Events with Secondary Vertex b-tagging", Winter 2006 public conference note.
  - [7] F. Abe, *et al.*, Nucl. Instrum. Methods Phys. Res. A **271**, 387 (1988); D. Amidei, *et al.*, Nucl. Instrum. Methods Phys. Res. A **350**, 73 (1994); F. Abe, *et al.*, Phys. Rev. D **52**, 4784 (1995); P. Azzi, *et al.*, Nucl. Instrum. Methods Phys. Res. A **360**, 137 (1995); The CDFII Detector Technical Design Report, Fermilab-Pub-96/390-E
  - [8] T. Sjostrand *et al.*, High-Energy-Physics Event Generation with PYTHIA 6.1, Comput. Phys. Commun. **135**, 238 (2001).
  - [9] M.L. Mangano *et al.*, JHEP **07**, 1 (2003).
  - [10] G. Corcella *et al.*, HERWIG 6: An Event Generator for Hadron Emission Reactions with Interfering Gluons (including supersymmetric processes), JHEP **01**, 10 (2001).
  - [11] H.L. Lai *et al.*, Eur. Phys. J. **C12**, 375 (200).
  - [12] CDF collaboration, "Measurement of the Cross Section for  $t\bar{t}$  Production Using Event Kinematics in  $p\bar{p}$  Collisions at  $1.96 \text{ TeV}$ ", CDF public note 8092.
  - [13] Lepton isolation is defined as the excess transverse energy in the calorimeter within a cone of radius 0.4 centred on the lepton direction, divided by the lepton transverse energy. The selection requirement is less than 10%.
  - [14] Brian D. Ripley, *Pattern recognition and Neural Networks*, Cambridge University Press (1996).
  - [15] Carsten Peterson, Thorsteinn Rögnvaldsson, Leif Lönnblad, *JETNET 3.0 - A Versatile Artificial Neural Network Package*, CERN-TH.7135/95.
  - [16] S. Klimentenko *et al.*, FERMILAB-FN-0741 (2003); D. Acosta *et al.*, Nucl. Instrum. Meth. **A494**, 57 (2002).

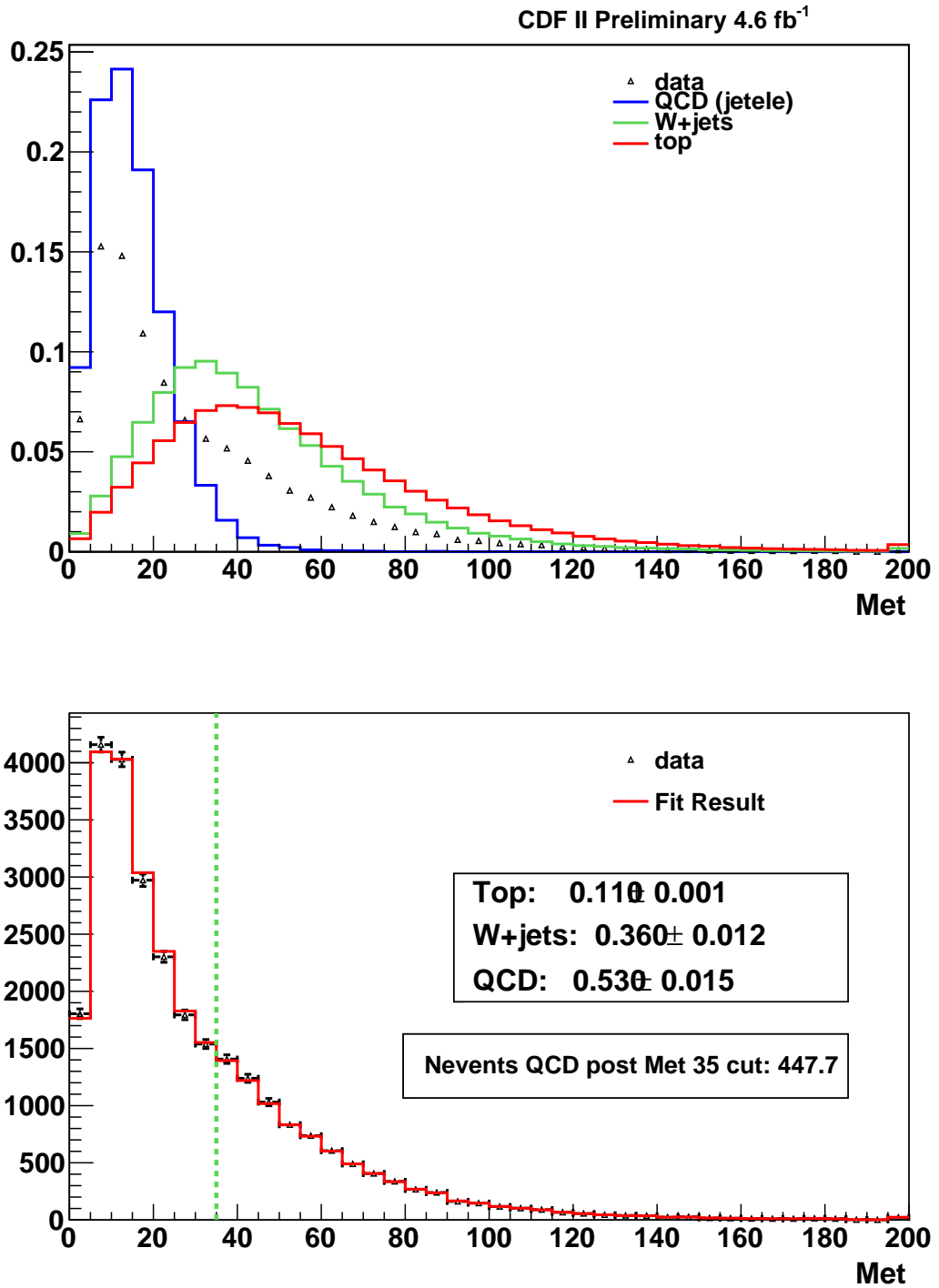


FIG. 1: (top)  $\cancel{E}_T$  templates for the data, top signal, W+jets and QCD backgrounds in the  $W+\geq 3$  jet case. These plots are normalised to unit area. (bottom) Comparison between the data and the fitted distribution. The fractions shown in the legend are before any  $\cancel{E}_T$  cut is applied.

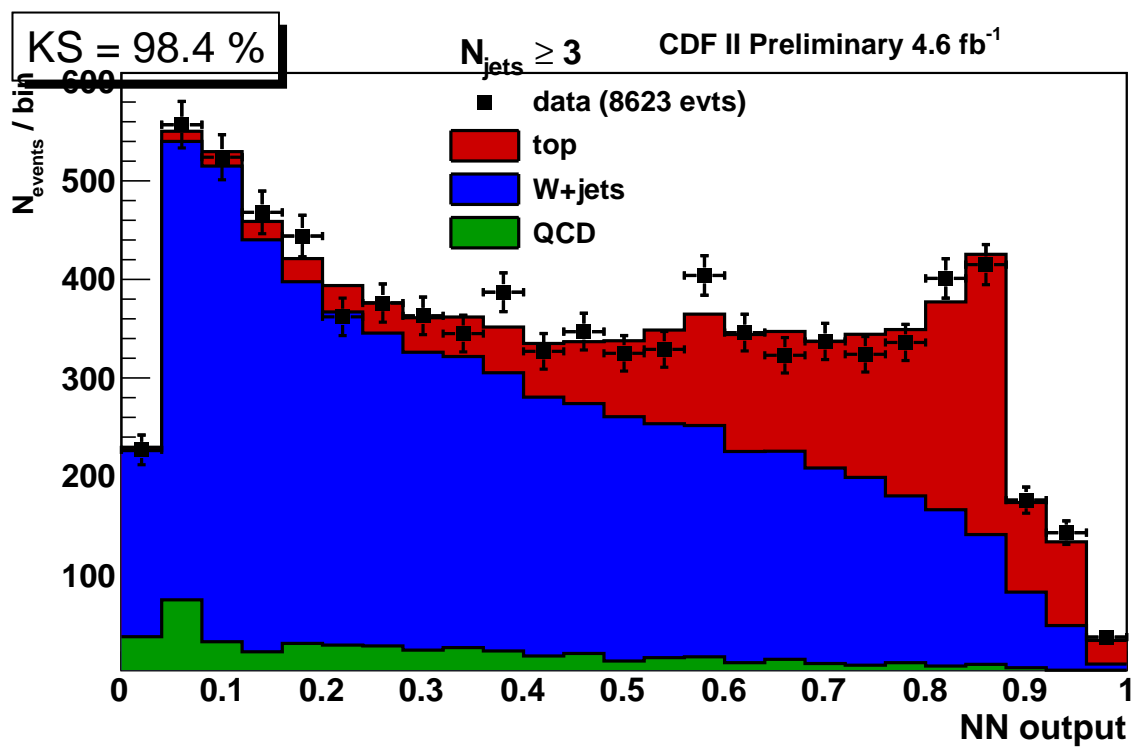


FIG. 2: NN output distribution in data (black points) compared to the fitted values for the signal (red) plus background (blue and green for W+jets and QCD, respectively).